3-D BAYESIAN ULTRASOUND BREAST IMAGE SEGMENTATION USING THE EM/MPM ALGORITHM

Lauren A. Christopher and Edward J. Delp†
Charles R. Meyer and Paul L. Carson‡

†Purdue University
Video and Image Processing Laboratory
School of Electrical and Computer Engineering
West Lafayette, IN 47907

‡The University of Michigan
Department of Radiology
Ann Arbor, MI 48109

ABSTRACT

In this paper, ultrasound breast image segmentation is improved by using the volumetric data available in neighboring slices. The new algorithm extends the EM/MPM framework to 3D by including pixels from neighboring frames in the Markov Random Field (MRF) clique. In addition, this paper describes a unique linear cost factor introduced in the optimization loop to compensate for the attenuation common to ultrasound images.

I. INTRODUCTION

Three-dimensional medical imaging has enjoyed wide application in the last decade. In addition to CT and MRI data, recent research reports an ultrasound volumetric image scan obtained by a single transducer array [1]. However, the best application of 3D imaging can be hampered by noise and other image processing problems. This is particularly true for ultrasound images, which have speckle noise caused by reflections from the sound wave and variations in attenuation through the tissue structures.

In addition to volumetric imaging, time sequential image scans can be composed into volumes. The work in [2][3][4] has allowed 3D volumes to be viewed from 2D image sequence sources, within and across imaging modalities (registration and compounding of CT and ultrasound data, for example). However, a major key to clinical interpretation of these 3D images is the segmentation problem. It takes many years of expertise for clinicians to accurately diagnose from an ultrasound image. Any assistance to this process is beneficial, such as automatic or semi-automatic segmentation.

Ultrasound is clearly a textured image, due to the speckle noise. Segmenting textures is a difficult task. Pioneering work by Besag [5] and Geman and Geman [6] created a framework for segmenting textures based on statistical analysis. The assumption made in these Bayesian techniques is that there is a "hidden" model that generates the observed image, and that model can be inferred using prior information. In addition, the concept of Markov Random Fields provides a 2D platform with which to estimate the best segmentation.

Some selected recent 2D applications of Bayesian techniques for texture segmentation in imaging are found in the following references. A multiscale segmentation technique on wavelet coefficients is found in [7]. A multiscale pyramid-filtered image segmentation is presented in [8]. In [9] an application of Bayesian segmentation to functional brain MRI images is described. Described in [10] is a multiscale application of Bayesian techniques to breast ultrasound images. In general, these techniques all use the maximum *a posteriori* (MAP) segmentation. Various algorithms are used to estimate the hyper-parameters (mean and variance of prior distributions).

This paper extends to 3D the work described in [11], combining EM algorithm for hyper-parameter estimation and Maximation of Posterior Marginals (MPM) algorithm for the segmentation. The benefit of MPM as described in [12] is an improved localized solution to the segmentation when compared with the MAP estimation. This is due to the fact that MPM assigns a cost to the number of incorrectly classified pixels, rather than optimizing for an overall average. In addition, the nested MPM loop can be used to provide the updates for the EM hyper-parameters [11].

Currently, an active area of research is the segmentation of 3D image data. A multiresolution Maximum *a posteriori* (MAP) segmentation for 3D data for *in vivo* cardiac ultrasound is shown in [13]. As in the 2D cases, this MAP estimation uses the Markov Random Field (MRF) Model, but extends it to a clique of 6-pixels in the neighborhood system. The hyper-parameters are

· Address all correspondence to E. J. Delp;
ace@ecn.purdue.edu

0-7803-7584-X/02/$17.00 ©2002 IEEE

estimated using textural (entropy, contrast, correlation, etc.) and acoustic (mean central frequency and integrated backscatter) features. In [14] a 3D MRF segmentation is performed on MRI images with the 6-pixel 3D clique. Then simulated annealing is used to converge to the best segmentation (in the MAP sense). Another 3D (MAP) segmentation is described in [15] of Brain MR images with training to obtain the hyper-parameters. Two MAP segmentation algorithms are compared, simulated annealing and Iterated Conditional Modes (ICM).

Our work, while also using the Bayesian MRF model and 6-pixel clique neighborhoods has several differences. The segmentation is performed with MPM and has the benefit of minimizing the misclassified pixels, as noted in [12]. The hyper-parameters, the means and variances of the gaussian prior models, are obtained iteratively with the EM algorithm, with the combined EM/MPM proof of convergence given in [11]. In our work, a computational reduction of the 3D is also proposed and demonstrated.

As described in [13], there is also an additional problem in ultrasound images, the attenuation across the (2D) image, corresponding to the depth of the scan. This is compensated for in our work by using a linearly varying cost factor in the MPM loop.

II. 3D-EM/MPM:

A. Statistical Motivation

We desire to estimate a "true image" given some corrupted observed image data. In the case of medical imaging, we want the true image to be a segmentation separating normal tissue from abnormal tissue. For the EM/MPM algorithm [11] and the MPM segmentation [12], this separation process takes the form of a "class label." We will assume that the "true image," X, can be modeled such that each pixel is a discrete random variable that takes on a discrete class label $\{1,2...,N\}$ with some probability mass function, and will be modeled as a Markov random field (MRF). We will denote the observed image that we want to segment as Y, whose pixels will be modeled as continuous random variables.

When a segmentation is generated, X is approximated by an estimate of X (here denoted $\hat{x}$). The MAP estimate is often used (using log likelihood) maximizing over x:

$$\hat{x} = \arg\max_x p_X(x \mid y) \qquad (1)$$

$$= \arg\max_x \left\{\log f_{Y|X}(y \mid x) + \log p_X(x)\right\} \qquad (2)$$

The Maximization of Posterior Marginals is shown in [12] to be equivalent to minimizing the Expectation of a cost function C, the cost of choosing the wrong class label. No cost is incurred when $X = \hat{x}$, cost for $X \neq \hat{x}$.

$$\hat{x} = \arg\min_x E\{C(X,\hat{x}) \mid Y = y\} \qquad (3)$$

So one can choose an appropriate cost function to match the Markov random field for X. This localized cost function depends on the neighborhood clique of pixels.

$$C_{MPM}(X,\hat{x}) = \sum_{s \in S} t(X_s - \hat{x}_s) \qquad (4)$$

s = current pixel; S = whole image

t = function of pixel neigborhood

The minimization in (3) is equivalent to maximizing [11][12]:

$$P(X_s = k \mid Y = y) \qquad (5)$$

over all k, where k is the class label. This is the maximization of the probability that the particular pixel X_s belongs to class label k, given the observed data.

The iterative solution is based on Markov random field theory and Gibbs Sampling, and is given a detailed account in [5] and [6].

B. 3-D Pixel Neighborhood, MRF, and MPM

The Markov random field (MRF) requires a "Clique", a pixel neighborhood system that is symmetric. The Clique used in this research contains the 4 closest pixels in the 2D neighborhood, and the pixels from the previous and next frames that are at the same 2D spatial co-ordinates. The pixel being segmented is denoted X_s and the neighborhood set of pixels is denoted X_r.

Making use of Gibbs sampling [6], the Probability Mass Function of X is:

$$p(x) = \frac{1}{Z}\exp\left(-\sum_{\{r,s\} \in C} \beta\, t(x_r, x_s) - \sum_{\{r\} \in C} \gamma_{x_r}\right) \qquad (6)$$

$$t(x_r, x_s) = \begin{pmatrix} 0; & x_r = x_s \\ 1; & x_r \neq x_s \end{pmatrix} \qquad C = \text{clique of } X$$

Z = normalizing value

β = weighting factor for amount of spatial interaction

γ_{x_r} = cost factor for class "k", used for ultrasound attenuation

A new application for γ is used in this research to remedy the effects of attenuation of ultrasound waves. A linearly increasing gamma is applied to the lower mean classes in order to compensate for the attenuation. An example is shown in the results section.

Samples of the observed image Y are assumed to be Random Variables distributed as i.i.d. Gaussian conditioned on the class label field (segmented image) X and sufficient statistics

$$\theta = \{\mu_1, {\sigma_1}^2 \mu_2, {\sigma_2}^2, ..., \mu_N, {\sigma_N}^2\}$$

of the N-fold Normal mixture distribution representing the observed data. Here we assume the number of classes N is known.

Combining into equation (1) we obtain the following function:

$$p(x \mid y,\theta) = \frac{f(y \mid x,\theta)p(x)}{f(y \mid \theta)}$$

$$= \frac{1}{f(y)}\left[\prod_{s=1}^{N} \frac{1}{\sqrt{2\pi\sigma_{x_s}^2}} \exp\left(-\frac{(y_s-\mu_{x_s})^2}{2\sigma_{x_s}^2}\right)\right]\left(\frac{1}{Z}\right)\exp(-\beta\, t(x_r,x_s)) \quad (7)$$

In [12] it is shown that the Markov Chain converged in probability to the distribution in (7). During the iterations of the Gibbs sampler, Marroquin showed that the estimate of equation (5) is the average number of times a pixel X_s spends in class label (k).

This paper introduces a new simplification for the 3D operation of MPM. Rather than optimizing over the entire volume space, this algorithm iterates 2D MPM on the previous and next frame of source image to create the class labels, and the current frame is optimized in 3D with these labels. This restricts the temporal influence of the segmentation to the nearest neighbors. For MPM, this is adequate.

C. Expectation-Maximization

The last part of the algorithm is the estimation of the Gaussian hyper-parameters θ . This is accomplished by the use of the Expectation-Maximization (EM) algorithm [16]. EM is well tailored for mixture distributions, where the algorithm estimates Maximum Likelihood (ML) of the hyper-parameters.

EM iterates through two steps. First the expectation step creates the current estimate of the hyper-parameters θ , then the maximization step, in our case: MPM. The expectation step requires the same statistics that MPM uses, namely the statistics used to maximize equation (5). Indexed by EM iteration "p" this Q function is maximized:

$$Q(\theta,\theta_{p-1}) = E\left[\log f(y \mid x,\theta) \mid Y,\theta_{p-1}\right] + E\left[\log p(x \mid \theta) \mid Y,\theta_{p-1}\right] \quad (8)$$

To find the θ_{p-1}, for each class k , the algorithm looks at the pixels that end up with class label k after the iterations of MPM. Then it computes the weighted average over the MPM iterations of the (changing) class means and variances. This is followed by a new EM maximization step entering the MPM loop with the new means and variances.

III. EXPERIMENTAL RESULTS :

A. 2D Segmentation

The first result of the research shows the improvement in segmentation by including a cost parameter γ to compensate for the attenuation of the ultrasound signal. In Figure (1) we show, segmented into 4 class labels, the ultrasound segmentation with and without γ applied to the two lowest mean class labels. This γ is linearly varied from top to bottom in the image, the slope determined by difference in the average brightness from the top to the bottom of the image. These segmentations were generated with $\beta = 3.2$, MPM-iteration (per EM)=3, and EM-iterations=250. In Figure 4(c) the γ class-cost parameter was applied linearly, top to bottom, on class[1] from 0 to 3, and class[2] from 0 to 2.5.

Here the black is the "background" segmentation, the next brighter level is the class of potential interest (for these breast ultrasounds it contains tumors, cysts, and fibroadenoma). In this case the top center structure is part of a 2x2x2cm carcinoma which required lumpectomy. The classification of the segmentation is not automatic. Some normal tissue appears also in this class. The brightest 2 classes in general are muscle and normal tissue.

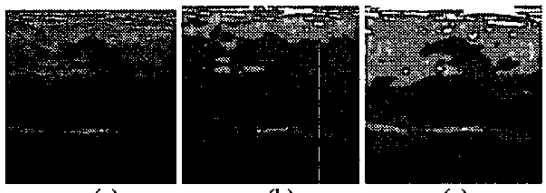

(a) (b) (c)

Figure (1) (a) Original Ultrasound (b) Uncompensated 2D EM-MPM segmentation (c) Gamma Compensated 2D EM-MPM segmentation

B. 3D Improvements

In ultrasound, a single 2D slice may be affected by reflection perpendicular to the wave incidence, causing speckle effects. For other types of imaging, such as CT, noise can affect an accurate 2D segmentation. Our results here show that including the third-dimension improves the segmentation of the 2D image, and also provides a more accurate representation of the 3D volume (as also reported in [14]).

Two images of the 3D ultrasound volume are presented here in Figure (2). The parameters for 3D are equivalent to the 2D case, as in part IIIA.

The 3D results reinforce the segmented image and produce a cleaner ultrasound by reducing the influence of one-frame only speckle noise. This is particularly true in the brightest segmentation class, white in above images.

CONCLUSIONS

This paper introduces the EM/MPM framework to 3D to improve segmentation of ultrasound images, and provides a 3-frame simplified algorithm for 3D. Additionally, the inclusion of a cost parameter γ inside the EM-MPM loop compensates the attenuation of ultrasound through tissue.

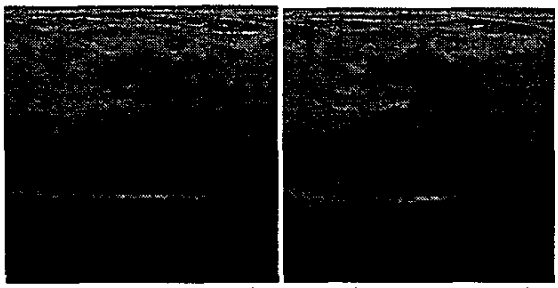

Figure (2a) Two consecutive source images, ultrasound

Figure (2b) 2D segmentation

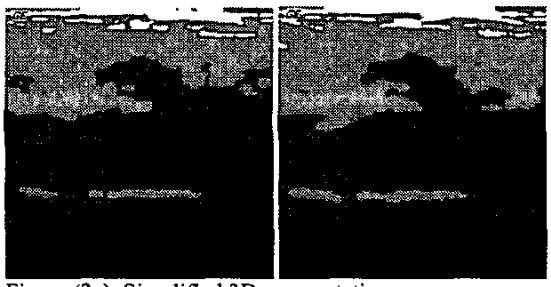

Figure (2c) Simplified 3D segmentation

References:

[1] J. T. Yen and S.W. Smith, "Real-Time Rectilinear Volumetric Imaging" *IEEE Transactions on Ultrasonics, Ferroelectronics and Frequency Control,* Vol. 49, No. 1, pp. 114-124, Jan. 2002

[2] J. F. Krucker, C. R. Meyer, G. L . LeCarpentier, J. B. Fowlkes, and P. L. Carson, "3D Spatial Compounding of Ultrasound Images Using Image-Based Nonrigid Registration" *Ultrasound in Medicine and Biology,* Vol. 26, No. 9, pp. 1475-1488, 2001

[3] C. R. Meyer, J. L. Boes, B. Kim, P. Bland, et al., "Demonstration of accuracy and clinical versatility of mutual information for automatic multimodality image fusion using affine and thin plate spline warped geometric deformations," *Medical Image Analysis*, vol. 3, pp. 195-206, 1997.

[4] A. Moskalik, P. L. Carson, C. R. Meyer, J. B. Fowlkes, J. M. Rubin and M. A. Roubidoux, "Registration of 3D Compound Ultrasound Scans of the Breast for Refraction and Motion Correction" *Ultrasound in Medicine and Biology,* Vol. 21, No. 6, pp. 769-778, 1995

[5] J. Besag, "Spatial interaction and the statistical analysis of lattice systems," *J. R. Stat. Soc. B,* Vol. 36, pp. 192-236, 1974.

[6] S. Geman and D. Geman, "Stochastic Relaxation, Gibbs Distributions, and the Bayesian Restoration of Images" *IEEE Transactions on Pattern Analysis and Machine Intelligence,* Vol. PAMI-6, No. 6, pp. 721-741, Nov. 1984

[7] H. Choi and R. Baraniuk "Multiscale Image Segmentation Using Wavelet-Domain Hidden Markov Models" *IEEE Transactions on Image Processing,* Vol. 10, no. 9, pp 1309-1321, Sept. 2001

[8] H. Cheng and C. Bouman, "Multiscale Bayesian Segmentation Using a Trainable Context Model", *IEEE Transactions on Image Processing,* Vol. 10, no. 4, pp 511-525, Apr. 2001

[9] J. Rajapakse and J. Piyaratna, "Bayesian Approach to Segmentation of Statistical Parametric Maps" *IEEE Transactions on Biomedical Engineering,* Vol. 48, no 10, pp. 1186-1194, Oct. 2001.

[10] D. Boukerroui et. al., "Multiresolution texture based adaptive clustering algorithm for breast lesion segmentation" *European Journal of Ultrasound 8 (1998)* p. 135-144

[11] M. L. Comer and E. J. Delp, "The EM/MPM Algorithm for Segmentation of Textured Images: Analysis and Further Experimental Results" *IEEE Transactions on Image Processing,* Vol. 9, No. 10, pp. 1731-1744, Oct. 2000

[12] J. Marroquin, S. Mitter, and T. Poggio, "Probabalistic solution of ill-posed problems in computational vision" *J. Amer. Statist. Assoc.,* vol 82, pp. 76-89, Mar. 1987.

[13] D. Boukerroui, O. Basset, A. Baskurt, G. Gimenez, "Multiparametric and Multiresolution Segmentation Algorithm of 3-D Ultrasonic Data" *IEEE Transactions on Ultrasonics, Ferroelectronics and Frequency Control,* Vol. 48, No. 1, pp. 64-76, Jan. 2001

[14] S. M. Choi, J. E. Lee, J. Kim, and M. H. Kim, "Volumetric Object Reconstruction Using the 3D-MRF Model-Based Segmentation" *IEEE Transactions on Medical Imaging,* Vol. 16, no. 6, pp. 887-892, Dec. 1997

[15] K. Held, E. R. Kops, B. J. Krause, W. M. Wells,III, R. Kikinis, and H. W. Muller-Gartner, "Markov Random field segmentation of brain MR images" *IEEE Transactions on Medical Imaging,* Vol. 16, no. 6, pp. 878-886,Dec. 1997

[16] T. Moon, "The Expectation-Maximization algorithm" *IEEE Signal Processing Magazine,* pp. 47-60, Nov. 1999.